◆ Human Brain Mapping 31:1297–1304 (2010) ◆

Layer-Specific BOLD Activation in Human V1

Peter J. Koopmans,[1]* Markus Barth,[1,2] and David G. Norris[1,2]

[1]*Radboud University Nijmegen, Donders Institute for Brain, Cognition and Behaviour, Nijmegen, The Netherlands*
[2]*University Duisburg-Essen, Erwin L. Hahn Institute for Magnetic Resonance Imaging, Essen, Germany*

Abstract: The neocortex is known to have a distinct laminar structure which has previously been probed in animals using high-resolution fMRI. Detection of layer-specific activation in humans has however to date proven elusive. In this study we demonstrate for the first time such layer-specific activation, specifically at a depth corresponding to layer IV of human primary visual cortex (V1). We used a gradient-echo (GE) sequence at 3T with an isotropic resolution of 0.75 mm, in which a stria at the depth of layer IV was visible in the averaged time series, and could be used as an anatomical landmark. Upon visual stimulation (7.5 Hz flickering checkerboard) the signal increase of 3% in layer IV was significantly higher than in the neighboring laminae. The width of this activation peak was 0.8–1 mm. Based on this result and known laminar organization of the intracortical vasculature we conclude that in the direction perpendicular to the cortical surface the intrinsic spatial resolution of the GE-BOLD fMRI signal is in the submillimetre range. Human laminar fMRI is a significant development which may improve our understanding of intracortical activation patterns and of the way in which different cortical regions interact. *Hum Brain Mapp 31:1297–1304, 2010.*

Key words: functional MRI; cortical layers; BOLD; BOLD spatial resolution; striate cortex; 3 Tesla

INTRODUCTION

The noninvasive measurement of hemodynamic responses to increased neural activity in the human brain at the resolution of the cortical layers by fMRI would offer unprecedented insights into brain function. For the first time it would be possible to examine the role of individual layers within a cortical region, and to relate layer-specific activity across regions. In this study we demonstrate layer specific activation in layer IV of human V1 at 3T in response to simple visual stimulation.

There is a body of literature on laminar activation profiles in animals using a range of fMRI techniques: arterial spin labelling (ASL) [Zappe et al., 2008], cerebral blood volume (CBV) weighted (using MION) [Harel et al., 2006; Lu et al., 2004; Smirnakis et al., 2007; Zhao et al., 2006], gradient-echo (GE) BOLD [Goense and Logothetis, 2006; Harel et al., 2006; Lu et al., 2004; Silva and Koretsky, 2002; Smirnakis et al., 2007; Zappe et al., 2008; Zhao et al., 2006] and spin-echo (SE) BOLD [Goense and Logothetis, 2006; Harel et al., 2006; Zhao et al., 2006]. To date, one GE study on humans has been reported [Ress et al., 2007].

The general pattern to emerge from these papers is that GE profiles show a monotonic increase in activity when going from white matter (WM) to cerebrospinal fluid (CSF) with a large, steep increase in activity near/at the surface (layer II and up) which is believed to be caused by superficial draining veins. Also, some of the studies show a slight increase in activation at layer IV [Goense and

Additional Supporting Information may be found in the online version of this article.

Contract grant sponsor: NWO; Contract grant number: ALW2PJ/04064.

*Correspondence to: Peter J. Koopmans, Radboud University Nijmegen, Donders Institute for Brain, Cognition and Behaviour, Nijmegen, The Netherlands. E-mail: peter.koopmans@donders.ru.nl

Received for publication 12 March 2009; Revised 2 September 2009; Accepted 7 October 2009

DOI: 10.1002/hbm.20936

Published online 15 January 2010 in Wiley Online Library (wileyonlinelibrary.com).

Logothetis, 2006; Harel et al., 2006] whereas this is absent in others [Ress et al., 2007; Zhao et al., 2006] complicating the interpretation of these layer-specific GE results.

In the SE results of [Goense and Logothetis, 2006; Harel et al., 2006] the peak in layer IV was much better visible than in the corresponding GE experiments. In Zhao et al. [2006] no peak was detected in the cat cortex even though the experimental setup was very similar to that used by Harel et al. [2006]. In all SE profiles the signal increase near the surface was far smaller than in the GE results. Goense and Logothetis [2006] showed that when decreasing the T_2^* weighting of the EPI readout train by increasing the number of segments, this peak near the surface could be reduced even further while the peak in layer IV remained.

Summarizing: although the literature on laminar fMRI is not entirely consistent, the perceived wisdom is that SE techniques offer improved localization because of their specific sensitivity to changes in the concentration of deoxyhemoglobin in the microvasculature as opposed to large draining veins which are more remote to the location of neuronal activation. This particularly holds at very high main magnetic field strengths (of 7T and above) where the contribution of the intravascular compartment to the SE signal diminishes markedly [Lee et al., 1999].

In order to decide which imaging technique should be employed in human laminar fMRI, some features of the neocortex have to be taken into account. Human neocortex is divided into six histological layers, and four vascular layers [Duvernoy et al., 1981]. (To improve clarity, throughout this paper the histological layers will be denoted in Roman numerals to distinguish them from the vascular layers.) The microvascular density is by far the greatest in vascular layer 3, which subsumes cortical layer IV which is known to be relatively thick in V1. In monkeys layer IV of V1 accounts for 26–36% of the cortical thickness [Preuss et al., 1999; Zheng et al., 1991] and in human V1 values are found between 26% [Preuss et al., 1999] and 42% [Eickhoff et al., 2007].

With regard to the sequence choice, it is likely that if a spin-echo sequence is employed its sensitivity will be biased towards vascular layer 3 compared with other vascular layers. Furthermore, a spin-echo sequence is less sensitive than a gradient-echo one. In SE two contrast mechanisms contribute to the BOLD signal as these effects can not be refocused with an RF pulse: intravascular T2 changes and extravascular dynamic dephasing effects (encountered around capillaries). In GE-BOLD the same mechanisms contribute along with two more: vascular dephasing (caused by the difference in susceptibility between a vein and its surrounding tissue) and static dephasing (encountered around veins larger than capillaries). At 3 Tesla the additional contrast mechanisms in GE-BOLD lead to a factor 3 sensitivity benefit with respect to SE-BOLD [Norris et al., 2002].

If a GE sequence is used, its spatial resolution may be compromised by the BOLD contribution of the pial veins at the cortical surface. However, following a similar argument to that in [Barth and Norris, 2007], we hypothesized that if we used a GE fMRI technique with both a high degree of anatomical trueness and very high, isotropic spatial resolution, then we would be able to eliminate the pial vein contributions on the basis of position alone.

With regard to the data analysis, another feature of the laminar structure of neocortex is important. Fatterpekar et al. [2002] used MR microscopy combined with histological staining to show that the relative depth of layer IV varies, depending on its position along the cortex. The thickness of layers V and VI reduces when going from the crowns of gyri to the troughs of sulci. This causes layer IV to shift from approximately halfway the cortical depth to very close to white matter. If one does not take this into account (by averaging sulci and gyri into one large region of interest (ROI) for instance) this can considerably blur laminar profiles of the deeper layers.

This study is hence constructed as follows: we investigate laminar activation profiles in GE fMRI data using small ROIs positioned along the banks of the sulci, thus avoiding troughs of sulci and crowns of gyri. These small (straight) ROIs made it possible to achieve precise localization of the laminar activation profiles by using the visible vascular layer 3/layer IV as an internal and independent reference. The pial vein contribution to these profiles was assessed by eliminating voxels identified by an automated vein segmentation filter.

MATERIALS AND METHODS

MR Data Acquisition

Seven subjects were scanned after informed consent was given according to the guidelines of the local ethics committee. Functional scans were acquired on a 3T Siemens Magnetom Trio system (Siemens, Erlangen, Germany) with a 3D FLASH sequence using a custom 8 channel occipital phased array coil (Stark Contrast, MRI Coils, Erlangen, Germany) [Barth and Norris, 2007]. Voxel size was $0.75 \times 0.75 \times 0.75$ mm^3, TR 35 ms, FA 15°, matrix size 256 $\times$ 256, 20 slices, readout bandwidth 130 Hz. GRAPPA [Griswold et al., 2002] was used for 4-fold acceleration along the inplane phase encoding direction (i.e. following the strip of coil elements). To optimize vein visibility, first order flow compensation was applied in all directions and TE was chosen to be 28 ms [Koopmans et al., 2008; Reichenbach et al., 2000]. As this study targeted primary visual cortex which is known to lie within the calcarine sulcus, the FOV was placed such that it covered as much of the sulcus as possible. Therefore the slab was positioned parallel to the calcarine sulcus i.e. the plane was tilted between transversal and coronal at a variable angle determined by the subject's anatomy.

The acquisition time per volume was 60 seconds, so the sequence has a poor temporal resolution and efficiency compared to conventional fMRI protocols. For future high

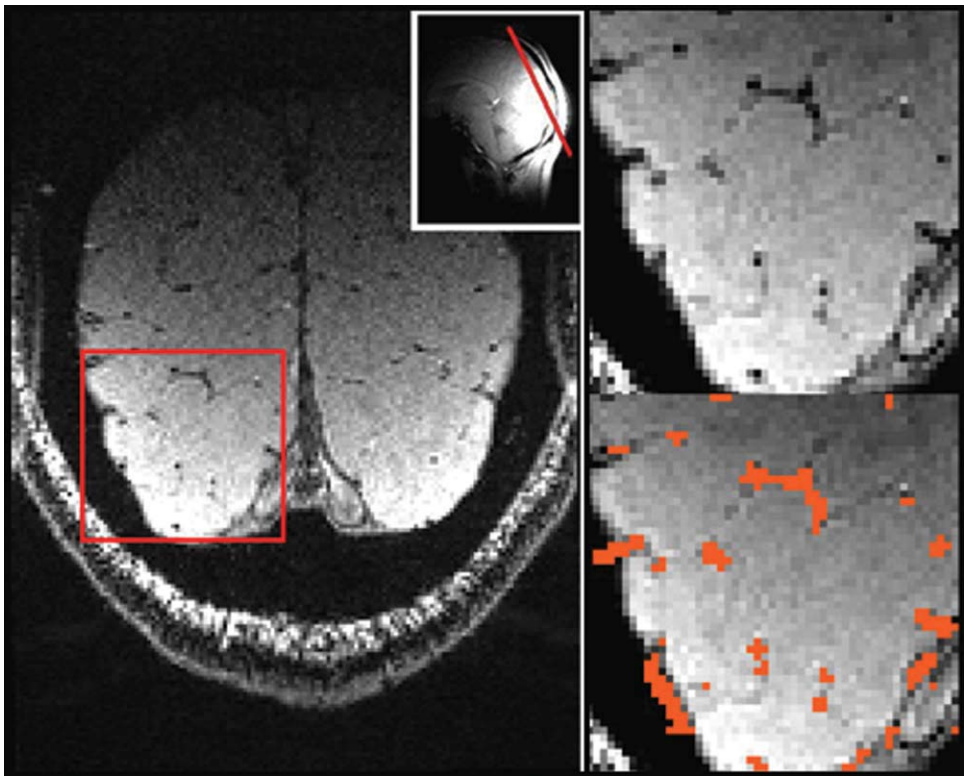

Figure 1.
Vein contrast. On the left a typical raw functional image is shown. Veins are clearly depicted as black dots. On the right a zoomed section of the visual cortex is shown. The orange overlay shows the automated vein segmentation results. [Color figure can be viewed in the online issue, which is available at wileyonlinelibrary.com.]

resolution GE studies, EPI would be a strong candidate to improve efficiency. The current approach however does offer a very good contrast between veins and brain tissue allowing for direct identification of the pial veins (see Fig. 1).

Visual stimulation consisted of a 7.5 Hz flashing checkerboard. In order to keep subjects' attention, a fixation cross that changed color every 5 seconds was included, and subjects responded to color changes by means of a button box. The rest condition consisted of a black screen including the fixation cross.

Functional experiments were accompanied by a T1-weighted MP-RAGE acquisition which had the same orientation, voxel size, bandwidth and FOV as the functional runs although 80 slices were scanned. Parameters were: TR 2300 ms, TI 1100 ms, TE 8 ms, FA 8°, BW 130 Hz. Acquisition time was 6 min.

Analysis

One dataset was eliminated because of gross subject motion between placing the FOV and the actual functional run resulting in a failure to cover the calcarine sulcus. Six datasets remained after elimination.

Realignment and Coregistration

Because of the spatial scales involved in the analysis, great care was taken during the realignment and coregistration steps to obtain high quality results. The functional data were realigned using SPM5 [Friston et al., 1995]. Due to the nature of the coil, a large and steep inhomogeneity gradient was present in the data. This could potentially affect realignment, therefore motion parameters were estimated on inhomogeneity corrected data. Because the fat on the scalp could change position with respect to the brain which severely degraded the quality of realignment, the parameters were estimated using a weighting volume. This weighting volume was a very smooth (FWHM ~16 mm) version of the inhomogeneous magnitude data with weighting factors outside the brain set to zero. The anatomical MP-RAGE volume was coregistered to the average functional volume, also using a weighting volume, which in this case was a binary brain mask (please note that minor modifications in the SPM5 coregistration code were required to be able to do this). All transformation parameters were calculated at the highest level of precision allowed by the software or hardware.

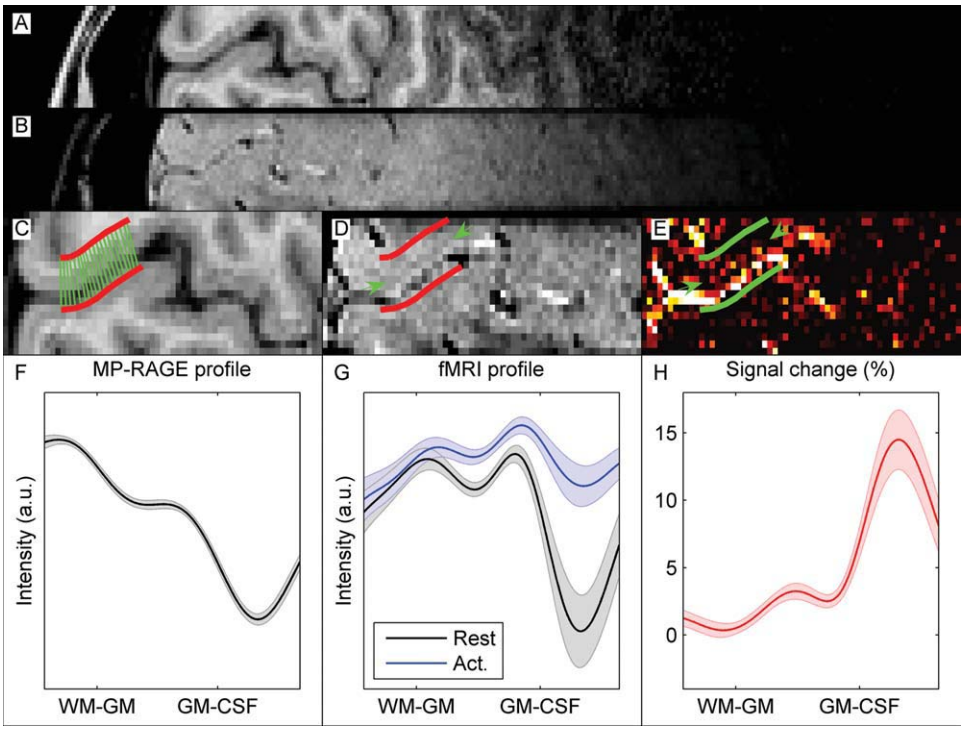

Figure 2.

Analysis method for a single subject. (**A**, **B**) Sagittal views of both MP-RAGE slab and the functional slab respectively. (**C**) Zoomed section of the image in (A) depicting the calcarine sulcus and the extent of the ROI (red lines). The green lines show the profile locations drawn across the ROI (not all are shown, in reality a profile is calculated every 0.075 mm). (**D**) Zoomed section of the image in (B), the green arrows indicate the intensity variation of vascular layer 3/layer IV. (**E**) *t*-map of visual stimulation versus rest, thresholded at a *t*-value of 1. The green arrows are at the same locations as in (D) pointing out the layer-specific activation. (**F**) The MP-RAGE profile averaged over slices and along the sulcus. (**G**) The average profile of both the rest (black) and the stimulated condition (blue). The dark band pointed out by the arrows in (D) is clearly visible in the profile. (**H**) Average profile of the relative signal change with respect to the GM intensity of the rest condition averaged across the entire cortical thickness in order to avoid biasing the profiles toward regions that are darker in the rest image (i.e., the dark band in the middle). In (F–H) the shading depicts estimated standard error of the mean. [Color figure can be viewed in the online issue, which is available at wileyonlinelibrary.com.]

Laminar Analysis

After motion correction the average functional volume revealed a dark band at the depth of layer IV. An interactive tool written in Matlab was used to draw initial profiles perpendicular to the cortex across these bands. The tool created additional profiles in between the ones drawn already, such that every 0.075 mm a profile was created. Data were interpolated using third-order sinc interpolation. Please note that care was taken that this interpolation step did not cause any ringing artefacts (see Supporting Information).

To decrease the amount of complexity in drawing the ROIs, the procedure was carried out in 2D only. Because of the FOV placement, sagittal cuts could be made which were approximately perpendicular to the calcarine sulcus in most subjects. This made it possible to copy the ROI to a slice above and below the original slice.

Within a slice, all profiles were plotted next to each other, effectively "unfolding" the cortex. To account for small shifts of the profiles between slices (because the sagittal cut was not *exactly* perpendicular to the sulcus), the slices were realigned by shifting them in the through-cortex direction using the stria as a reference. Average profiles per subject were created by collapsing the unfolded images along the cortex direction for both the stimulated condition and the rest condition as well as for the MP-RAGE images. This was required to overcome the SNR reduction due to the high resolution used. The procedure, yielding one profile per subject is depicted for a single subject in Figure 2.

In each subject's profile, the positions of the WM/GM and the GM/CSF interfaces were manually determined using both the MP-RAGE and the functional data. The profiles were then normalized based upon their cortical thickness before averaging across subjects. The average

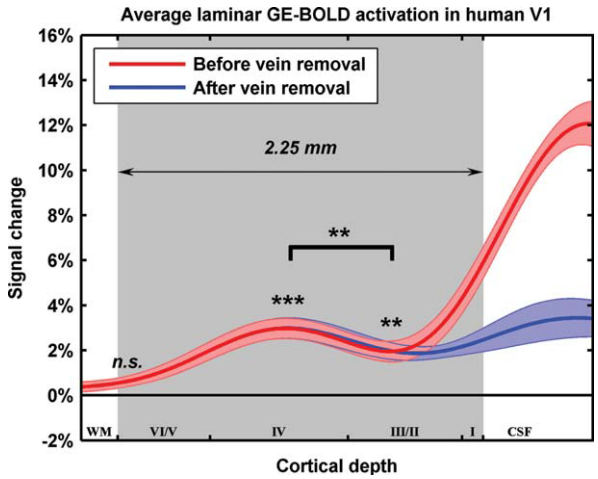

Figure 3.

Average laminar activation profile in human V1. The red curve shows the laminar activation before venous voxel removal. The shading shows standard error of the mean. Layer IV is significantly more activated than the supragranular layers which themselves are also significantly activated (**$P < 0.01$; ***$P < 0.001$). The blue profile shows the same curve after removal of venous voxels. Although some activation near the surface remains (see Discussion) a large reduction can be seen. The gray shading denotes GM which had an average thickness of 2.3 $\pm$ 0.2 mm. The distribution of the layers (*x*-axis) was taken from stains of human V1 published in [Preuss et al., 1999]. [Color figure can be viewed in the online issue, which is available at wileyonlinelibrary.com.]

activation profile is shown in red in Figure 3. The distribution of the layers in this Figure 3 (x-axis) was taken from stains of human V1 published in Preuss et al. [1999].

Vessel Filtering

The functional images clearly show extracortical veins which appear as dark spots throughout the brain (Fig. 1). Manual segmentation of these veins is a tedious process and in earlier work [Koopmans et al., 2008] we showed results of an automated vein segmentation routine. In short, the segmentation filter detects veins based upon the local second order structure of the image. Performance of the filtering is improved by iteratively performing vessel detection followed by anisotropic filtering of the data and repeating these steps a number of times. We refer to Koopmans et al. [2008] for further details. The result of the exclusion of voxels containing visible veins is shown in blue in Figure 3.

RESULTS AND DISCUSSION

As mentioned above, ROIs were defined in each subject on a patch of straight cortex (i.e. not in troughs of sulci or crowns of gyri) containing a dark band at the cortical depth of layer IV. The average ROI size was 95 $\pm$ 36 mm^3. Figure 2 shows the ROI-based results for one of the six subjects. Panels A and B show a single sagittal slice of the anatomical and the average functional rest volume, respectively. Panels C and D are zoomed sections of A and B. The thick red lines show the extent of the ROI. The green lines in C represent the location of the profiles drawn across GM (only a subset is shown for visualization purposes). The arrows in D point to the dark band at the depth of layer IV. Panel E shows *t*-scores of visual stimulation versus rest, thresholded at a value of 1. Apart from the high values at the surface, increased activation in the dark band can be seen (depicted by the green arrows). Panels F, G and H show the average cortical profiles over three sagittal slices of the MP-RAGE, functional volume and relative signal change, respectively. The shaded areas depict estimated standard error of the mean. The activation shown in H is calculated as a relative signal change with respect to the GM intensity averaged across the entire cortical thickness in order to avoid biasing the relative signal change profiles toward regions that are darker in the rest image (i.e. the dark band in the middle).

In all subjects, a large signal change at the surface was seen. More interestingly however, a peak was also seen at the depth corresponding to layer IV. The results correspond excellently to the SE results found in monkeys [Goense and Logothetis, 2006] and in cats [Harel et al., 2006]. As both these papers argue that their activation is localized to layer IV, by extension it is hence highly plausible that the activation in the current study arises from this layer.

In order to investigate this layer-specific result in more detail, the average activation profile of all subjects is shown in Figure 3. The layer IV activation peaks at 3% signal change and is significantly higher than the activation in the more superficial layers II/III.

Before interpreting these results it is important to eliminate the possibility this is due to systematic errors causing an artifact to show up in all subjects. Two relevant options would be Gibbs ringing and ringing due to the interpolation necessary to generate profiles perpendicular to the cortical surface. These effects are assessed and reported in the Supporting Information section. In short: Gibbs ringing can not explain the visibility of layer IV as a consequence of a sharp intensity edge at the surface caused by low intensity CSF/vein signals. In regions where the sharp edge near the surface is not present (where two banks of a sulcus are pushed against one another for instance), layer IV is still visible. The analysis in the Supporting Information shows that the visibilities of the layer and of the edge are not correlated making a Gibbs ringing explanation for the laminar activation impossible. The fact that interpolation ringing is not causing layer IV to appear is shown by re-evaluating the data using nearest-neighbor interpolation. This method is intrinsically ringing-free and the curve obtained still shows the layer.

Laminar Resolution of GE-BOLD

Despite intra- and intersubject variability the FWHM of the layer IV peak in Figure 3 was approximately 0.8–1 mm corresponding to 40% of the cortical thickness. Such submillimetre resolution usually is only considered to be possible in GE-BOLD with differential stimuli in which activation conditions are closely matched. This causes the activation in the pial veins to disappear in the subtractions (a method frequently used in retinotopy and ocular dominance column studies). This line of thought however is focused on the spread of activation *along* the cortical surface (i.e. tangentially) not *through* the cortex (i.e. radially).

Based upon figures in Duvernoy et al. [1981], we hypothesize that the through-cortex BOLD resolution (for both SE and GE) will be much more forgiving in terms of laminar studies than the "classical" one measured along the cortical surface. The first reason for this is that Duvernoy reported that small collecting veins (parallel to the cortex) starting in the capillary bed in a particular layer, are "confined" to a relatively narrow laminar band before they reach one of the larger (30–100 μm) intracortical draining veins which run perpendicular to the cortex. This means that *inside* the cortex, i.e. excluding pial vessels, the tangential, non-differential resolution will be of the order of the diameter of the vascular unit of 0.75–4 mm [Lauwers et al., 2008], but the radial resolution should maximally be of the order of 100 μm, as estimated by taking twice the mean capillary length [Lauwers et al., 2008] (Please note that this factor 2 results from a worst case scenario estimation, i.e. the capillaries are oriented either straight to WM or straight toward the surface.) Of course, this theoretical radial resolution is reduced by the perpendicular draining veins, to which GE is also sensitive. However, these veins show uni-directional flow towards the cortical surface only. This means that the laminar spread of activation could be asymmetrical. Because this spread would have a relatively steep flank at the WM side, the ability to detect layer-specific activation within the cortex could therefore be conserved (provided the resolution of the measurement is not dominated by the voxel size). An important further consideration for our experiments is that the classical, non-differential GE-BOLD point-spread function as reported in e.g. Parkes et al. [2005] is largely determined by the *extracortical* draining veins that lead away from the activated area [Barth and Norris, 2007] and can go beyond the diameter of the vascular unit. In our experiment, these pial veins do not degrade the laminar resolution as they only influence the profiles near the surface as was shown by eliminating venous voxels.

Eliminating Venous Contribution

Figure 3 shows the profiles averaged over subjects before (red) and after (blue) removal of veins. Although only 12% ± 6% of the voxels in the ROI were removed the signal increase near the surface is markedly reduced. This indicates that the signal increase in the superficial layers is predominantly caused by signal changes in large draining veins and does indeed not reflect "true" increased neuronal activity.

After vein removal, the profiles still showed some increase at the surface. This is likely to be caused by the fact that only veins of a certain (unknown) minimum diameter will be detected. Smaller draining veins will still contribute to the activation profiles. It should be noted that this minimum diameter can be much smaller than the voxel size used. The venous contrast in the sequence is (among other effects) based upon the intra-voxel dephasing between blood and other tissue, lowering that voxel's intensity. As long as the signal reduction with respect to the surrounding voxels is large enough, the voxel will be segmented as a vein and both the vein and the surrounding tissue contained in the voxel will be removed from the analysis [Barth and Norris, 2007].

The remaining signal increase near the pial surface could in theory also be explained by the fact that removing a vein does not remove all the extravascular effect that vein has on its surroundings. In this study however it is unlikely to cause the increase near the surface as the profile does not change when the voxels neighboring the veins are also removed (data not shown).

We conclude that although pial vein contributions clearly affect GE measurements relatively close to the cortical surface, vein segmentation and subsequent removal helps reducing the effect while the deeper layers are not affected. This allows for reliable functional imaging of at least the non-superficial layers.

Origin of the Layer-Specific Signal

The origin of the layer IV specific peak found here and by others has been subject of debate, one of the reasons for this being that it is not always detected. As mentioned in the Introduction, the differences between SE experimental setups of Harel et al. [2006] and Zhao et al. [2006] seem very small, but the resulting profiles are very different. The same holds for the GE experiments reported in these articles. The cause(s) of these discrepancies are not obvious.

Another problem is that there does not seem to be an obvious reason why the activation to checkerboard or moving grating stimuli should be stronger in layer IV. A possible explanation for the stronger activation in layer IV may be given by recurrent circuits mentioned further down in this discussion.

It is well known that the capillary density in layer IV is simply higher than in other layers and especially SE but to a lesser extent also GE profiles will be biased by this. In Lauwers et al. [2008] capillary density profiles are given as a possible explanation for SE activation profiles and similar arguments were made concerning total blood volume and GE activation profiles. On the other hand, in Goense

and Logothetis [2006] and Harel et al. [2006] arguments are made against this being the only possibility. The capillary density may be highest in layer IV, it is very high still in layers II and III (as can be seen in Fig. 59 in Duvernoy et al. [1981]). This is not reflected in spin-echo laminar activation profiles measured. Furthermore, [Harel et al., 2006] found that although the capillary density profiles in cats are very similar in area 17 and 18, the layer IV specific effect was mainly found in area 18. The fact that CBV-weighted laminar studies typically report much broader peaks including parts of layer II and V [Harel et al., 2006; Smirnakis et al., 2007; Zhao et al., 2006] makes it unlikely that the layer IV specific GE-BOLD response is caused solely by blood volume variations.

A final argument can be found in a study by [Bissig and Berkowitz, 2009]. Here rats were systematically injected with $MnCl_2$ for 8 hours while visually stimulated with moving gratings. Mn^{2+} enters active neurons through voltage-gated Calcium channels, but the Mn^{2+} efflux is very slow, making it possible to image the integral of previous neural activity some hours later. Of the many brain regions analysed, only layer IV and the top third of layer V in primary visual cortex and the optic nerve layer of the superior colliculus showed significant differences in activation compared to rats that had not been exposed to the stimulus. As this method relies on Manganese uptake by activated neurons as opposed to hemodynamic responses it suggests that layer IV specific activation in V1 can not solely be explained by vascular distributions.

An explanation alternative to vascular distributions could be found in the underlying neuronal laminar structure of the cortex. Upon activation three physiological effects contribute to the BOLD effect: increased cerebral blood flow (CBF) leads to a positive BOLD response, increased CBV and oxygen metabolism both lead to a negative BOLD effect. The layer-specific signal increase reported here, suggests that changes in blood flow upon activation are regulated at the laminar level as an increase in blood flow at the level of the pial arteries should lead to an increased BOLD effect in all layers. This is compatible with layer IV specific CBF activation in ASL measurements [Zappe et al., 2008] and findings in [Caesar et al., 2003; Gerrits et al., 2000; Norup Nielsen and Lauritzen, 2001; Silva and Koretsky, 2002] where evidence was found in favor of a laminar-specific regulation of CBF. Combined electrophysiology-BOLD studies have shown the BOLD effect to be more strongly correlated to input and local processing (LFPs) than to output (spiking rate) [Caesar et al., 2003; Logothetis et al., 2001]. Also, the input layer IV is known to consist of densely packed spiny stellate cells. As only 10% of the excitatory synapses in layer IV originate from the LGN [Ahmed et al., 1994], these stellate cells are thought to be involved in recurrent excitation circuits acting as amplifiers [Douglas et al., 1995]. They have been shown to have a significant influence in the regulation of cerebral blood flow ([Attwell and Iadecola, 2002] and refs therein) and could therefore possibly explain the local blood flow increase leading to a layer-specific, positive BOLD response.

Summarizing, it is hard to untangle layer-specific BOLD results from local capillary density or blood volume profiles as metabolic demand correlates strongly with vascular density [Borowsky and Collins, 1989]. However, the current literature does not support an explanation of the signal changes in layer IV solely on the basis of vascular density arguments. This leaves an underlying neurovascular coupling mechanism as a highly plausible alternative.

With respect to high resolution fMRI sensitivity issues it is of great relevance that GE has been shown to be capable to depict layer-specific activation when averaging over a patch of cortex. We have shown that when the signal of extracortical veins is removed then the effective resolution of laminar fMRI is in the submillimetre range. Furthermore, as GE is intrinsically (3-5 times) more sensitive than SE [Boxerman et al., 1995], GE seems to be the method of choice for laminar studies in humans although higher field strengths and more efficient pulse sequences remain to be explored. Our results show that fMRI can study the human brain at the laminar level, giving a level of unprecedented spatial specificity previously only possible in animal studies.

ACKNOWLEDGMENTS

The authors thank Benedikt Poser for critically reading the article.

REFERENCES

Ahmed B, Anderson JC, Douglas RJ, Martin KA, Nelson JC (1994): Polyneuronal innervation of spiny stellate neurons in cat visual cortex. J Comp Neurol 341:39–49.

Attwell D, Iadecola C (2002): The neural basis of functional brain imaging signals. Trends Neurosci 25:621–625.

Barth M, Norris DG (2007): Very high-resolution three-dimensional functional MRI of the human visual cortex with elimination of large venous vessels. NMR Biomed 20:477–484.

Bissig D, Berkowitz BA (2009): Manganese-enhanced MRI of layer-specific activity in the visual cortex from awake and free-moving rats. Neuroimage 44:627–635.

Borowsky IW, Collins RC (1989): Metabolic anatomy of brain: a comparison of regional capillary density, glucose metabolism, and enzyme activities. J Comp Neurol 288:401–413.

Boxerman JL, Hamberg LM, Rosen BR, Weisskoff RM (1995): MR contrast due to intravascular magnetic susceptibility perturbations. Magn Reson Med 34:555–566.

Caesar K, Gold L, Lauritzen M (2003): Context sensitivity of activity-dependent increases in cerebral blood flow. Proc Natl Acad Sci USA 100:4239–4244.

Douglas RJ, Koch C, Mahowald M, Martin KA, Suarez HH (1995): Recurrent excitation in neocortical circuits. Science 269:981–985.

Duvernoy HM, Delon S, Vannson JL (1981): Cortical blood vessels of the human brain. Brain Res Bull 7:519–579.

Eickhoff SB, Rottschy C, Zilles K (2007): Laminar distribution and co-distribution of neurotransmitter receptors in early human visual cortex. Brain Struct Funct 212:255–267.

Fatterpekar GM, Naidich TP, Delman BN, Aguinaldo JG, Gultekin SH, Sherwood CC, Hof PR, Drayer BP, Fayad ZA (2002): Cytoarchitecture of the human cerebral cortex: MR microscopy of excised specimens at 9.4 Tesla. AJNR Am J Neuroradiol 23:1313–1321.

Friston KJ, Ashburner J, Frith CD, Poline JB, Heather JD, Frackowiak RSJ (1995): Spatial registration and normalization of images. Hum Brain Mapp 3:165–189.

Gerrits RJ, Raczynski C, Greene AS, Stein EA (2000): Regional cerebral blood flow responses to variable frequency whisker stimulation: an autoradiographic analysis. Brain Res 864:205–212.

Goense JB, Logothetis NK (2006): Laminar specificity in monkey V1 using high-resolution SE-fMRI. Magn Reson Imaging 24:381–392.

Griswold MA, Jakob PM, Heidemann RM, Nittka M, Jellus V, Wang J, Kiefer B, Haase A (2002): Generalized autocalibrating partially parallel acquisitions (GRAPPA). Magn Reson Med 47:1202–1210.

Harel N, Lin J, Moeller S, Ugurbil K, Yacoub E (2006): Combined imaging-histological study of cortical laminar specificity of fMRI signals. Neuroimage 29:879–887.

Koopmans PJ, Manniesing R, Niessen WJ, Viergever MA, Barth M (2008): MR venography of the human brain using susceptibility weighted imaging at very high field strength. Magn Reson Mater Phy 21:149–158.

Lauwers F, Cassot F, Lauwers-Cances V, Puwanarajah P, Duvernoy H (2008): Morphometry of the human cerebral cortex microcirculation: general characteristics and space-related profiles. Neuroimage 39:936–948.

Lee SP, Silva AC, Ugurbil K, Kim SG (1999): Diffusion-weighted spin-echo fMRI at 9.4 T: microvascular/tissue contribution to BOLD signal changes. Magn Reson Med 42:919–928.

Logothetis NK, Pauls J, Augath M, Trinath T, Oeltermann A (2001): Neurophysiological investigation of the basis of the fMRI signal. Nature 412:150–157.

Lu H, Patel S, Luo F, Li SJ, Hillard CJ, Ward BD, Hyde JS (2004): Spatial correlations of laminar BOLD and CBV responses to rat whisker stimulation with neuronal activity localized by Fos expression. Magn Reson Med 52:1060–1068.

Norris DG, Zysset S, Mildner T, Wiggins CJ (2002): An investigation of the value of spin-echo-based fMRI using a Stroop color-word matching task and EPI at 3 T. Neuroimage 15:719–726.

Norup Nielsen A, Lauritzen M. (2001): Coupling and uncoupling of activity-dependent increases of neuronal activity and blood flow in rat somatosensory cortex. J Physiol 533:773–785.

Parkes LM, Schwarzbach JV, Bouts AA, Deckers RH, Pullens P, Kerskens CM, Norris DG (2005): Quantifying the spatial resolution of the gradient echo and spin echo BOLD response at 3 Tesla. Magn Reson Med 54:1465–1472.

Preuss TM, Qi H, Kaas JH (1999): Distinctive compartmental organization of human primary visual cortex. Proc Natl Acad Sci USA 96:11601–11606.

Reichenbach JR, Barth M, Haacke EM, Klarhofer M, Kaiser WA, Moser E (2000): High-resolution MR venography at 3.0 Tesla. J Comput Assist Tomogr 24:949–957.

Ress D, Glover GH, Liu J, Wandell B (2007): Laminar profiles of functional activity in the human brain. Neuroimage 34:74–84.

Silva AC, Koretsky AP (2002): Laminar specificity of functional MRI onset times during somatosensory stimulation in rat. Proc Natl Acad Sci USA 99:15182–15187.

Smirnakis SM, Schmid MC, Weber B, Tolias AS, Augath M, Logothetis NK (2007): Spatial specificity of BOLD versus cerebral blood volume fMRI for mapping cortical organization. J Cereb Blood Flow Metab 27:1248–1261.

Zappe AC, Pfeuffer J, Merkle H, Logothetis NK, Goense JB (2008): The effect of labeling parameters on perfusion-based fMRI in nonhuman primates. J Cereb Blood Flow Metab 28:640–652.

Zhao F, Wang P, Hendrich K, Ugurbil K, Kim SG (2006): Cortical layer-dependent BOLD and CBV responses measured by spin-echo and gradient-echo fMRI: insights into hemodynamic regulation. Neuroimage 30:1149–1160.

Zheng D, LaMantia AS, Purves D (1991): Specialized vascularization of the primate visual cortex. J Neurosci 11:2622–2629.